Chemical Science

EDGE ARTICLE

View Article Online
View Journal | View Issue

Cite this: *Chem. Sci.*, 2014, **5**, 4851

Interaction and reactivity of synthetic aminoisoflavones with metal-free and metal-associated amyloid-β†

Alaina S. DeToma,‡[a] Janarthanan Krishnamoorthy,‡[ab] Younwoo Nam,[cde] Hyuck Jin Lee,[ae] Jeffrey R. Brender,[ab] Akiko Kochi,[ae] Dongkuk Lee,[d] Valentina Onnis,[f] Cenzo Congiu,[f] Stefano Manfredini,[g] Silvia Vertuani,[g] Gianfranco Balboni,*[f] Ayyalusamy Ramamoorthy*[ab] and Mi Hee Lim*[ce]

Metal ion homeostasis in conjunction with amyloid-β (Aβ) aggregation in the brain has been implicated in Alzheimer's disease (AD) pathogenesis. To uncover the interplay between metal ions and Aβ peptides, synthetic, multifunctional small molecules have been employed to modulate Aβ aggregation *in vitro*. Naturally occurring flavonoids have emerged as a valuable class of compounds for this purpose due to their ability to control both metal-free and metal-induced Aβ aggregation. Although flavonoids have shown anti-amyloidogenic effects, the structural moieties of flavonoids responsible for such reactivity have not been fully identified. In order to understand the structure–interaction–reactivity relationship within the flavonoid family for metal-free and metal-associated Aβ, we designed, synthesized, and characterized a set of isoflavone derivatives, aminoisoflavones (**1–4**), that displayed reactivity (*i.e.*, modulation of Aβ aggregation) *in vitro*. NMR studies revealed a potential binding site for aminoisoflavones between the N-terminal loop and central helix of prefibrillar Aβ, which is different from the non-specific binding observed for other flavonoids. The absence or presence of the catechol group, responsible for metal binding, differentiated the binding affinities of aminoisoflavones with Aβ and enthalpy/entropy balance for their Aβ interaction. Furthermore, having a catechol group influenced the binding mode with fibrillar Aβ. Inclusion of additional substituents moderately tuned the impact of aminoisoflavones on Aβ aggregation. Overall, through these studies, we obtained valuable insights into the requirements for parity among metal chelation, intermolecular interactions, and substituent variation for Aβ interaction.

Received 24th May 2014
Accepted 1st August 2014

DOI: 10.1039/c4sc01531b

www.rsc.org/chemicalscience

Introduction

Alzheimer's disease (AD) is rapidly becoming one of the most prominent public health concerns worldwide, especially due to the present lack of a curative treatment.[1] AD is commonly classified as a protein misfolding disease due to the observation of proteinaceous aggregates in diseased brain tissue, including senile plaques and neurofibrillary tangles.[1b–e,2] The primary components of the senile plaques are aggregated forms of amyloid-β (Aβ) peptides.[1b–e,3] Self-association of monomeric Aβ into various amyloid assemblies produces neurotoxic species, leading to AD pathogenesis;[4] however, plaques can have a heterogeneous composition, with other components identified in the deposits. For example, metal ions have been found in association with the plaques and could be linked to neurotoxicity in AD.[1d,e,2c,5]

Cu(I/II), Zn(II), and more recently Fe(II), have been shown to bind to Aβ peptides *in vitro*.[1b–e,2c,5e,f,6,7] Furthermore, Cu(II)- and Zn(II)-bound Aβ peptides have been found to aggregate more rapidly than their metal-free counterparts.[8] It has also been proposed that redox active metal ions, such as Cu(I/II), bound to Aβ could participate in redox cycling, leading to an overproduction of reactive oxygen species (ROS) and, subsequently, elevated oxidative stress.[5c,d,9] As metal binding to Aβ may have multiple potential consequences, consideration of the direct

[a]*Department of Chemistry, University of Michigan, Ann Arbor, Michigan 48109-1055, USA*

[b]*Biophysics, University of Michigan, Ann Arbor, Michigan 48109-1055, USA. E-mail: ramamoor@umich.edu*

[c]*Life Sciences Institute, University of Michigan, Ann Arbor, Michigan 48109-2216, USA*

[d]*Department of Fine Chemistry, Seoul National University of Science and Technology, Seoul, Korea*

[e]*Department of Chemistry, Ulsan National Institute of Science and Technology (UNIST), Ulsan 689-798, Korea. E-mail: mhlim@unist.ac.kr*

[f]*Department of Life and Environmental Sciences, Pharmaceutical, Pharmacological and Nutraceutical Sciences Unit, University of Cagliari, I-09124 Cagliari, Italy. E-mail: gbalboni@unica.it*

[g]*Department of Life Sciences and Biotechnology, University of Ferrara, I-44121 Ferrara, Italy*

† Electronic supplementary information (ESI) available: Table S1 and Fig. S1–S11. See DOI: 10.1039/c4sc01531b

‡ These authors contributed equally.

interaction between these metal ions and Aβ peptides as a pathological factor is warranted; however, little evidence has been accumulated to clarify the involvement of metal-associated Aβ (metal–Aβ) species *in vivo* and their contribution to AD.

In the attempt to explore the connection between metal–Aβ species and AD, employing small molecules as chemical tools may be useful. For this purpose, there have been increasing efforts to probe Cu(II)–Aβ and Zn(II)–Aβ *in vitro* using compounds with specific structural moieties for simultaneous interaction with metal ions and Aβ (*i.e.*, bifunctionality).[1b,c,10] The majority of molecules have been designed by direct modification of known Aβ plaque imaging agents.[10a–c,11] In the incorporation design approach, heteroatoms for metal chelation are directly installed into the imaging agent framework.[10,11] This design strategy affords several advantages for future applications, including careful selection of moieties that could facilitate brain uptake and appropriate tuning of metal binding affinity to avoid systemic metal chelation and disruption of metal ion homeostasis in the brain.[1b,10a,b] Although several compounds with bifunctionality have provided useful insights into the reactivity of metal–Aβ, there remains much to be understood about these molecules' functions at the molecular level and the impact of their structural features on their interaction and reactivity with metal-free and metal–Aβ species. Rational screening or selection of natural products has identified flavonoids as a source of suitable chemical structures for such investigation and modification.[12] Flavonoids are plant-derived compounds that have been studied in models of inflammation, cancer, oxidative stress, and dementia.[13] Initially, myricetin (Fig. 1a) was found to modulate metal-mediated Aβ aggregation and neurotoxicity *in vitro* due to its metal chelation and Aβ interaction properties.[12a] More recently, the influence of (−)-epigallocatechin-3-gallate (EGCG, Fig. 1a) on both metal-free and metal-induced Aβ aggregation was characterized in detail at the molecular level.[12b] EGCG bound to metal–Aβ was able to alter Aβ conformation; off-pathway Aβ aggregation occurred leading to amorphous Aβ aggregates.[12b,14] This outcome represents an additional path by which the formation of toxic oligomeric Aβ intermediates may be circumvented. In order to reconcile the previously reported findings using myricetin and EGCG with the rational design approach, it would be worthwhile to identify the essential structural moieties within a flavonoid framework required to target metal-free and metal-associated Aβ species and modulate their reactivity, which will offer small molecule candidates as chemical tools for studying Aβ and metal–Aβ species.

Herein, we report the design and preparation of simple flavonoid derivatives, aminoisoflavones (**1–4**, Fig. 1b), with the intention of merging the qualities attained from rational-based design strategy into the isoflavone framework, which is known to contain auspicious biological characteristics toward AD (*vide infra*);[13a,15] along with a detailed evaluation of their Cu(II), Zn(II), and Aβ interaction properties for understanding their ability to regulate metal-free and metal-induced Aβ aggregation. Our overall results and observations demonstrate that deconstruction of naturally occurring flavonoids for redesign with selective inclusion of only a few functional groups is sufficient to effectively target metal ions, Aβ, and metal–Aβ and to subsequently control Aβ aggregation *in vitro*. Moreover, structural modification of the isoflavone framework, chosen for its synthetically friendly scaffold, does not diminish its innate beneficial traits toward AD-related reactivity. Using our aminoisoflavone derivatives, the foundation of a structure–interaction–reactivity relationship for flavonoids toward metal-free and metal-associated Aβ is strengthened by detailed characterization of their properties at the molecular level.

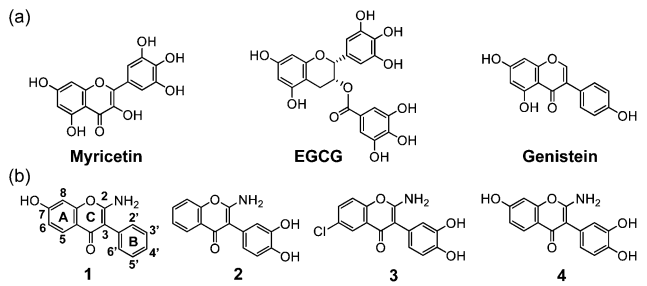

Fig. 1 Chemical structures of (a) naturally occurring flavonoids (myricetin, EGCG, and genistein) and (b) synthetic aminoisoflavones (**1–4**). (a) Left to right: myricetin: 3,5,7-trihydroxy-2-(3,4,5-trihydroxyphenyl)-4*H*-chromen-4-one; EGCG: (−)-epigallocatechin-3-gallate or (2*R*,3*R*)-5,7-dihydroxy-2-(3,4,5-trihydroxyphenyl)chroman-3-yl-3,4,5-trihydroxybenzoate; genistein: 5,7-dihydroxy-3-(4-hydroxyphenyl)-4*H*-chromen-4-one. (b) Left to right: **1**: 2-amino-7-hydroxy-3-phenyl-4*H*-chromen-4-one; **2**: 2-amino-3-(3,4-dihydroxyphenyl)-4*H*-chromen-4-one; **3**: 2-amino-6-chloro-3-(3,4-dihydroxyphenyl)-4*H*-chromen-4-one; **4**: 2-amino-3-(3,4-dihydroxyphenyl)-7-hydroxy-4*H*-chromen-4-one.

Results and discussion

Design and synthesis of aminoisoflavone derivatives

In the search for small molecules to interrogate the relationship between metal ions and Aβ species, selection of naturally occurring flavonoids has offered a new avenue for chemical tool development due to their multiple targeting capabilities, which may include various enzymes and ROS.[12,16] Recognizing that certain structural moieties are common to natural flavonoids (*e.g.*, catechol group; potentially for metal binding), a new family of synthetic flavonoids, aminoisoflavones (**1–4**, Fig. 1b) with tractable structural modifications were designed and prepared. Although the coordination chemistry of catechol and its corresponding metal complexes is well known,[17] knowledge of its role in flavonoid derivatives for targeting and modulating metal-free and metal-induced Aβ aggregation has received little attention. Additionally, incorporation of an amine functionality (*e.g.*, NH_2) could be used to gauge the tolerance of the framework to unnatural substituents,[18] which might be useful for tuning the metal binding and/or Aβ interaction properties by rational structure-based modifications in later stages.

The aminoisoflavones are derived from the structures of soy isoflavones, such as genistein (Fig. 1a), which are known to have multiple biological effects, and they have been employed as Aβ aggregation inhibitors and as neuroprotective molecules.[15] Synthetic aminoisoflavone derivatives have been demonstrated

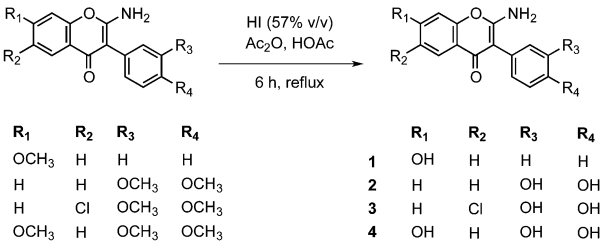

	R_1	R_2	R_3	R_4
1a	OCH_3	H	H	H
2a	H	H	OCH_3	OCH_3
3a	H	Cl	OCH_3	OCH_3
4a	OCH_3	H	OCH_3	OCH_3

	R_1	R_2	R_3	R_4
1	OH	H	H	H
2	H	H	OH	OH
3	H	Cl	OH	OH
4	OH	H	OH	OH

Scheme 1 Synthetic route to **1–4**.

previously to have inhibitory activity against various isoforms of human carbonic anhydrase (hCAI and hCAII),[19] a metalloenzyme that has been occasionally linked to AD.[20] Thus, we were curious to know whether the family of compounds could target and modulate another aspect of AD-related reactivity. The design of the new aminoisoflavones **1–4** (Fig. 1b) involves the *o*-dihydroxy moiety (*i.e.*, catechol) for metal chelation in **2**, **3**, and **4** and substituents, such as OH or Cl, in the A ring to modify the electronics or sterics of the molecules to influence their reactivity with Aβ or metal–Aβ (*vide infra*). Compound **1** was prepared as an analogue of **4** that lacks the catechol group, for comparison of interaction and reactivity with metal ions, Aβ, and metal–Aβ. The design further employs a primary amine in the 2 position of the C ring within the core framework of the isoflavone, which may be beneficial for improving solubility compared to naturally occurring flavonoids (Fig. 1).[18] The inclusion of the amine group is also related to the design of Aβ plaque imaging agents and multifunctional small molecules that have used amine derivatives to interact with the peptide.[11a–d,i,21] Among them, a dimethylamino functionality has been commonly used for targeting Aβ aggregates; however, the reported derivatives containing a primary amine can also enable interaction with the peptide.[11d] The aminoisoflavones (**1–4**) presented here are synthesized by acidic cleavage of the methoxylated aminoisoflavone precursors,[19b] and they were obtained in relatively high yield (76–86%) (Scheme 1). The multiple structural aspects of these aminoisoflavones, including the isoflavone framework, the catechol motif, and the primary amine, make them attractive candidates for detailed characterization of their chemical properties and their subsequent influence on metal-free and metal-induced Aβ aggregation *in vitro*.

Aβ aggregation in the absence and presence of aminoisoflavones

The extent to which the aminoisoflavones could control Aβ aggregation (inhibition experiment; Fig. 2) or alter preformed Aβ aggregates (disaggregation experiment; Fig. S1†) in the absence and presence of Cu(II) and Zn(II) was investigated.[10g–l,o,p,12a,b,22] For both studies, gel electrophoresis with Western blot was used to visualize the molecular weight (MW) distribution of the resulting Aβ species; transmission electron microscopy (TEM) was employed to detect their morphologies.

In the inhibition experiment, differences in the reactivity of compounds were observed toward both metal-free and metal-induced Aβ aggregation (Fig. 2). Reactivity of compounds is inferred by the ability of the compound to control the peptide aggregation pathway; aiming to generate Aβ species with a wide distribution of MW which are soluble to penetrate the gel matrix. All of the aminoisoflavones were able to modulate metal-free $A\beta_{40}$ aggregation as evidenced by the range of various-sized Aβ species visualized (Fig. 2a, lanes 1–4) in comparison to compound-free Aβ (lane C). In the presence of Cu(II) or Zn(II), however, varying degrees of ability to control metal-triggered $A\beta_{40}$ aggregation were observed. Cu(II)- or Zn(II)-mediated $A\beta_{40}$ aggregation was influenced by the catechol containing compounds (**2**, **3**, and **4**), but not by **1**, mainly generating $A\beta_{40}$ species having MW $\leq$ 75 kDa (lanes 2–4), which may indicate the redirection of Aβ aggregation as previously described for flavonoids.[12b,14,23,24] Fewer high MW gel-permeable aggregates were detected with **2** in comparison to that of **3** and **4** (lanes 2–4), which may represent a modest effect from the inclusion of the additional substituents (*i.e.*, Cl, OH) that are present in the A ring for **3** and **4** on peptide aggregation relative to the unsubstituted analogue **2** (Fig. 1b). Unstructured, amorphous Aβ aggregates were shown in previous reports;[12b,14,23,24] similarly, TEM images of Cu(II)- and Zn(II)-added Aβ samples treated with **4** revealed smaller-sized, amorphous species, while larger Aβ aggregates were observed with compound-untreated metal–Aβ samples (Fig. 2). In contrast, metal-free Aβ samples added with **4** displayed structured Aβ aggregates similar to those of compound-free $A\beta_{40}$. In addition, minimal morphological changes were exhibited upon treatment with **1** for both metal-free and metal-treated conditions, suggesting that **1** may interact with metal-free and metal-associated Aβ species differently from **4**.

Furthermore, in order to understand the structural moieties that could play a role in the control of Aβ aggregation, the reactivity of catechol (a metal binding site in **2–4**) and a mixture of **1** (flavonoid only) and catechol, with both metal-free and metal-associated $A\beta_{40}$, was investigated (Fig. S2†). In metal-free conditions, some reactivity toward $A\beta_{40}$ was only observed for **1** or a mixture of **1** and catechol (Fig. S2†, lanes 2 and 4), implying that the structural framework of **1**, and not catechol, may be important for metal-free $A\beta_{40}$ aggregation. In the case of metal-induced $A\beta_{40}$ aggregation, no reactivity was indicated with **1** (lane 2), while noticeable reactivity was displayed with metal–Aβ treated with catechol or a mixture of **1** and catechol (lanes 3 and 4). Moreover, the reactivity of the mixture of **1** and catechol was more distinguishable toward Cu(II)–$A\beta_{40}$, in comparison to that of catechol, similar to that shown by **2–4**. On the other hand, Zn(II)-induced $A\beta_{40}$ aggregation was less modulated by catechol and a mixture of **1** and catechol than **2–4**. These observations suggest that the catechol moiety and the fragment equivalent to **1** within the structural framework of **2–4** could be important for interaction with metal–$A\beta_{40}$ and metal-free $A\beta_{40}$, respectively; however, the ability of **2–4** to control metal-free and metal-induced $A\beta_{40}$ aggregation is driven by their overall structure (not by individual structural components).

It is also relevant to consider the reactivity of these ligands with $A\beta_{42}$, which has been suggested to primarily compose the senile plaques and found to aggregate *via* different

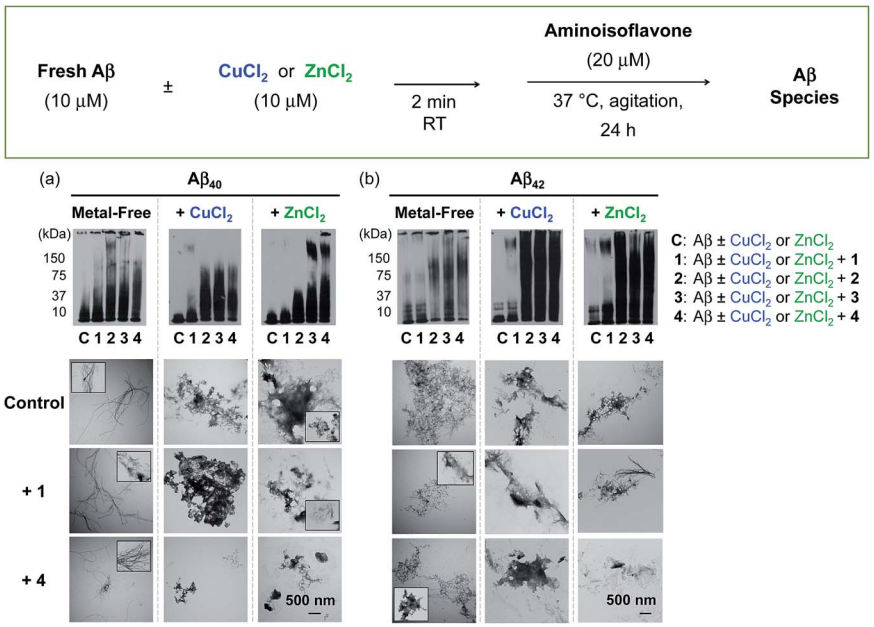

Fig. 2 Investigation of the ability of **1–4** to modulate the formation of metal-free and metal-induced $A\beta_{40}$ and $A\beta_{42}$ aggregates. Top: scheme of the inhibition experiment. Middle: analysis of the samples including (a) $A\beta_{40}$ and (b) $A\beta_{42}$ by gel electrophoresis followed by Western blot (6E10). Lanes: (C) Aβ ± $CuCl_2$ or $ZnCl_2$ (C = control), (1) C + **1**; (2) C + **2**; (3) C + **3**; (4) C + **4**. Bottom: TEM images of samples with **1** or **4** with (a) $A\beta_{40}$ or (b) $A\beta_{42}$. Experimental conditions: [$A\beta_{40}$ or $A\beta_{42}$] = 10 μM; [$CuCl_2$ or $ZnCl_2$] = 10 μM; [aminoisoflavone] = 20 μM; 1% v/v DMSO; 20 mM HEPES, pH 7.4, 150 mM NaCl; 24 h; 37 °C; agitation.

intermediates in comparison to $A\beta_{40}$.[1e,2b,3b,25] Overall patterns observed for $A\beta_{42}$ were similar to those for $A\beta_{40}$ in the inhibition experiment (*vide supra*; Fig. 2). Metal-free $A\beta_{42}$ aggregation was moderately influenced by **2**, **3**, and **4**, to a lesser extent by **1** (Fig. 2b, lanes 1–4). In samples containing metal ions, **2**, **3**, and **4** showed analogously greater reactivity, over metal-free conditions, visualized by the darker intensity of gel bands suggesting that all three compounds may alter metal-induced $A\beta_{42}$ aggregation in a similar fashion (lanes 2–4). Noticeably less reactivity was indicated with **1** in either metal-free or metal-triggered $A\beta_{42}$ aggregation. From the TEM results, mixtures of large, amorphous $A\beta_{42}$ species were observed in metal-free and metal-treated conditions upon the treatment of **4** in comparison to compound-untreated metal-free or metal–Aβ which presented structured $A\beta_{42}$ aggregates.

The aminoisoflavones were also evaluated for their ability to transform preformed metal-free or metal-associated $A\beta_{40}$ or $A\beta_{42}$ aggregates (Fig. S1†). Overall, the reactivity patterns of the compounds observed in the disaggregation experiments were similar to those of the inhibition experiment. In samples containing Aβ, metal ions, and **2**, **3**, or **4** (lanes 2–4), different distribution patterns were exhibited in comparison to those of compound-free conditions (lanes C). In contrast to inhibition results, minimal reactivity was observed upon the treatment of metal-free $A\beta_{40}$ aggregates with **1**, **2**, **3**, or **4** (lanes 1–4). Different from **1**, metal chelation *via* the catechol moiety in **2**, **3**, and **4**, could likely play a role in redirecting preformed metal–$A\beta_{42}$ aggregates. The TEM results showed a mixture of different-sized amorphous Aβ aggregates upon the treatment of either metal-free or metal-induced Aβ species with **4**, while more structured Aβ aggregates were present for compound-untreated samples under the same conditions (Fig. S1†).

Furthermore, the methoxylated precursors of **1**, **2**, and **4** (*i.e.*, **1a**, **2a**, and **4a**, respectively; Scheme 1) were also studied in order to determine the potential role of the catechol moiety in the reactivity of aminoisoflavones toward metal-free/-induced Aβ aggregation. As depicted in Fig. S3†, a very minimal effect of **1a**, **2a**, or **4a** was observed with Cu(II)–$A\beta_{40}$ in both inhibition and disaggregation experiments. In all scenarios, **1a**, **2a**, or **4a** did not affect metal-free or Zn(II)-mediated $A\beta_{40/42}$ aggregation. Taken together, our inhibition and disaggregation results reveal the scope of flavonoid derivatives that can be used to modulate metal-free and metal-induced Aβ aggregation and validate the requirement for sufficient metal binding and Aβ interaction properties to suitably influence this reactivity. The absence of the metal chelation moiety, catechol, in **1** as well as in **1a**, **2a**, or **4a** hindered the modulation of metal-induced $A\beta_{40/42}$ aggregation, implying that the catechol moiety may be a key factor in the reactivity of aminoisoflavones with metal–Aβ species. Moreover, additional substituents on the A ring (*i.e.*, Cl for **3** and OH for **4**) may also influence the regulation of Aβ aggregation.

Solution speciation studies of aminoisoflavones

The acidity constants (pK_a) for the aminoisoflavones were determined by variable-pH spectrophotometric titrations (I = 0.1 M, room temperature) following previously reported procedures (Fig. 3).[10f,h–l,o,p,26] The primary amine common to all four aminoisoflavones was assigned to the most acidic pK_a values, consistent with the predicted values for these structures.[27]

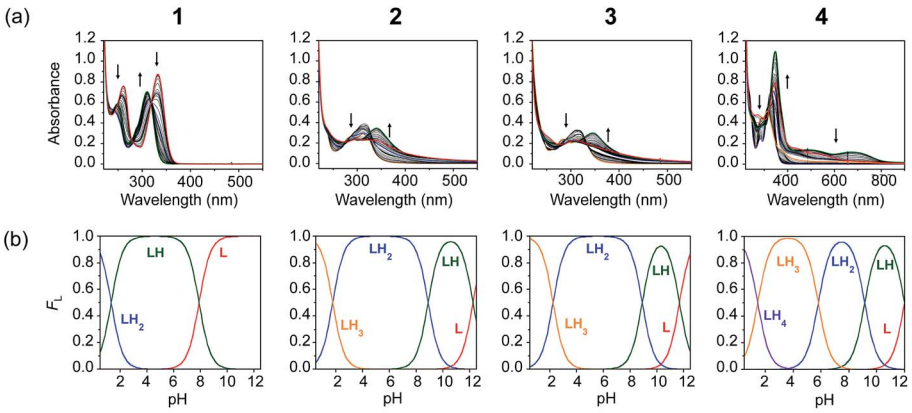

(c)

							pK$_a$[a]			
							1	2	3	4
LH_4	⇌	LH_3	+	H		(pK_{a1})	–	–	–	1.5(4)
LH_3	⇌	LH_2	+	H		(pK_{a2})	–	1.8(5)	2.2(9)	5.8(3)
LH_2	⇌	LH	+	H		(pK_{a3})	1.3(1)	8.9(2)	8.9(3)	9.1(2)
LH	⇌	L	+	H		(pK_{a4})	7.9(1)	12.3(4)	11.7(2)	12.0(2)

Fig. 3 Solution speciation studies of **1–4**. (a) Variable-pH UV-Vis titration spectra and (b) solution speciation diagrams for **1–4** (F_L = fraction of species in solution). (c) Summary of solution equilibria and acidity constants. Experimental conditions: [**1** or **4**] = 30 μM, [**2**] = 20 μM, [**3**] = 15 μM; I = 0.1 M NaCl; room temperature. Charges are omitted for clarity. [a] The error in the last digit is shown in parentheses.

Deprotonation of the ammonium (RNH_3^+) to the primary amine (RNH_2) was represented by pK_a values of 1.3 ± 0.1 for **1**, 1.8 ± 0.5 for **2**, 2.2 ± 0.9 for **3**, and 1.5 ± 0.4 for **4**. With the exception of **1**, each of the structures contains a catechol moiety, which had expected pK_a values of *ca.* 9 and 13 for the hydroxyl groups.[17a–c] The pK_a values for the catechol/catecholate equilibrium were 8.9 ± 0.2 and 12.3 ± 0.4 for **2**; 8.9 ± 0.3 and 11.7 ± 0.2 for **3**; 9.1 ± 0.2 and 12.0 ± 0.2 for **4**, with the more basic pK_a value corresponding to deprotonation of the hydroxyl group in the *para* position.[17a–c] An additional pK_a value corresponding to deprotonation of the hydroxyl substituent on the A ring in **1** and **4** was 7.9 ± 0.1 and 5.8 ± 0.3, respectively.

Based on these pK_a values, speciation diagrams were drawn to illustrate the fraction of ligand protonation states at each pH in solution. Each ligand would exist mainly in its fully deprotonated form above pH 12 (*i.e.*, L), and would have an overall negative charge. At pH 7.4, the dominant species is expected to be neutral for **1** (LH), **2** (LH_2), and **3** (LH_2), and monodeprotonated for **4** (LH_2). For future applications of these molecules, neutral species would be favored for facilitating brain uptake *via* passive diffusion across the blood–brain barrier (BBB).[28] Furthermore, characterization of the species distribution could be valuable for rationalizing the metal–Aβ binding properties for these molecules, as described below.

Metal binding studies

The aminoisoflavones **2**, **3**, and **4** were designed to be capable of metal binding *via* a catechol group, similar to other polyphenols.[12a,b,29] The catechol moiety is a prevalent ligand in biology, appearing in naturally occurring molecules, such as flavonoids, and in neurotransmitters (*e.g.*, dopamine, epinephrine).[17b,30] Known to be a strong metal chelator, the inclusion of this functionality in the aminoisoflavone framework was anticipated to interact with metal ions surrounded by the Aβ species.[17b,c,31] The Cu(II) and Zn(II) binding properties of the aminoisoflavones were investigated initially by UV-Vis, in the absence and presence of $Aβ_{40}$ (Fig. S4–S6†). More detailed Cu(II) binding properties were also characterized by variable-pH UV-Vis titrations. Upon incubation of the aminoisoflavones **2**, **3**, and **4** (20 μM, 1% v/v DMSO) with $CuCl_2$ in an aqueous buffered solution (20 mM HEPES, pH 7.4, 150 mM NaCl), differences in the optical spectrum of the free ligand were observed (Fig. S4†). With 0.5 equiv. of $CuCl_2$, new absorption features at *ca.* 480 nm were detected; additionally, prolonged incubation of the solution resulted in the appearance of a broad feature centered at *ca.* 800 nm.[32] Subsequent addition of $CuCl_2$ enhanced the intensity of these peaks (Fig. S4†). Note that the peak at *ca.* 800 nm was not observed from the solutions containing only the aminoisoflavones, suggesting the involvement of Cu(II) in that optical feature. No noticeable changes in the optical spectra were observed with **1**, which lacks the catechol group (Fig. S4†).

Zn(II) binding to the aminoisoflavones was also investigated by UV-Vis. It should be noted that the ligand concentration was increased to a ten-fold excess (*i.e.*, 100 μM) relative to $ZnCl_2$ (10 μM) in order to monitor an optical change upon metal binding (Fig. S5†). Similar to the Cu(II) binding data, addition of Zn(II) had no effect on the spectrum of **1** (Fig. S5a†). There were also no substantial changes for **3** with Zn(II); however, **2** and **4** showed new features in the UV-Vis spectra after *ca.* 12–24 h incubation. For **2**, an increase in the peak at *ca.* 285 nm and a shift to *ca.* 390 nm were observed (Fig. S5b†). Similarly, **4** displayed a progressive bathochromic shift from *ca.* 320 nm to 350

nm over 24 h (Fig. S5d†). These spectral variations could be indicative of partial deprotonation of the hydroxyl groups upon Zn(II) binding.[30] This partial ligand deprotonation might also cause a weak, broad feature around 800 nm that is similar to, but less intense than, that of the Cu(II) binding spectra.[32] This observation correlates to the Cu(II) speciation results at pH 7.4 detailed below, which suggests partial deprotonation of the catechol upon metal binding.[17b,30] Thus, deprotonation of **4** from LH_2 to LH form may occur upon Zn(II) binding to some extent.

To investigate whether the aminoisoflavones might bind to metal ions in the presence of Aβ, UV-Vis studies were conducted with $Aβ_{40}$, $CuCl_2$, and **4** (Fig. S6†). The titration experiments were performed by two different means. First, $Aβ_{40}$ (10 μM) was incubated with $CuCl_2$ for 5 min, followed by **4**. Second, Aβ was added into the resulting solution generated after 5 min incubation of **4** with $CuCl_2$ (Fig. S6†). Both solutions were titrated to result in final [Aβ] : [$CuCl_2$] : [**4**] ratios of 1 : 0.5 : 2, 1 : 1 : 2, 1 : 2 : 2, or 1 : 4 : 2. The condition using a 1 : 1 : 2 ratio was representative of the concentrations used in the *in vitro* aggregation studies (*vide supra*), and the resulting Cu(II) binding spectra in the presence of Aβ were observed to have similar features as those acquired without peptide present for both titration experiments (Fig. S4 and S6†). In the conditions using substoichiometric Cu(II) relative to Aβ, it was presumed that the amount of free Cu(II) in solution was minimal.[1b–e,5f] Incubation of **4** with the solution of Aβ and Cu(II) produced changes in the spectra, which was similarly observed when Aβ was introduced to a solution of **4** and Cu(II). Addition of **4** to the Cu(II)-treated Aβ solution suggests potential Cu(II)–**4** complex formation; furthermore, the presence of a Cu(II)–**4** complex was still apparent upon the addition of Aβ to the **4**-/Cu(II) solution (Fig. S6†), which implies that this compound may possibly compete with Aβ as a ligand for Cu(II).

Overall, these investigations demonstrate binding of the catechol-containing aminoisoflavone derivatives to Cu(II) and Zn(II). The solutions containing Cu(II) and the aminoisoflavones generated a unique optical feature, dominated by a low intensity transition bordering on the near-infrared (IR) region of the spectrum. This feature could correspond to changes in the electronic structure leading to a charge transfer process that populates a lower energy transition, as has been observed for different ligand frameworks.[33] Another possibility is that this feature represents a radical intermediate that was generated upon metal binding.[17f,34,28,30] It has been well established that deprotonated catechol participates in an equilibrium that involves the partially oxidized semiquinone and fully oxidized quinone.[17f] In the presence of divalent cations (*e.g.*, Cu(II)), this process might involve concomitant reduction of Cu(II) to Cu(I), while forming an oxidized ligand intermediate.[17b,f,35] In a few cases, however, Cu(II)–semiquinone complexes have been reported; most of these complexes are relatively colorless ($\varepsilon_{800} \approx 500\ M^{-1}\ cm^{-1}$) and are paramagnetic.[32,36] To advance the understanding of the Cu(II) binding properties of the aminoisoflavones, **4** was used as a model ligand for further investigations.

Stability constants (log β) and the dissociation constants (K_d) of Cu(II)–**4** complexes in solution (1 : 2 [Cu(II)]/[**4**], I = 0.1 M, room temperature; pH 4–7) were determined by variable-pH UV-Vis titration experiments (Fig. 4).[10f,h,j–l,o,p,26] Based on the calculated log β values, a solution speciation diagram was generated and indicated a mixture of Cu(II)–**4** complexes in 1 : 1 and 1 : 2 Cu(II)/ligand ratios. As depicted in Fig. 4, at pH 7.4, Cu(LH) existed relatively predominantly (*ca.* 80%; LH represents the monoprotonated form of **4** where the hydroxyl group in the *para* position of the B ring is protonated). There were additional species present at pH 7.4, such as $Cu(LH)_2$ (*ca.* 18%) and $Cu(LH_2)$ (*ca.* 2%). As indicated in Fig. 4, from titration, the solution was mainly 1 : 1 complexes below pH 7 (*i.e.*, Cu(LH), $Cu(LH_2)$, $Cu(LH_3)$). From this model, **4** was found to have high binding affinity for Cu(II), estimated based on the free Cu(II) concentration measured at a given pH (*i.e.*, pCu = $-\log[Cu(II)_{unchelated}]$).[10f,h,k,l,o,p,26] At pH 7.4, which was used for the *in vitro* experiments and is physiologically relevant, the pCu value for **4** was *ca.* 17, suggesting an estimated K_d for Cu(II)–**4** in the lower femtomolar range. The estimated K_d value for **4** to Cu(II) is slightly stronger than most reported K_d values for Cu(II)–Aβ peptides (*i.e.*, nanomolar to picomolar) and could be used to rationalize the potential partial chelation of Cu(II) by **4** in the presence of Aβ observed by UV-Vis (Fig. S6†; *vide supra*).[1b–e,5e,f] Along with the Cu(II) binding studies in the presence of Aβ (Fig. S6†), these data represent the possibility that **4** and other catechol-containing aminoisoflavone compounds (*e.g.*, **2**, **3**) could be competitive ligands for Cu(II) with Aβ.

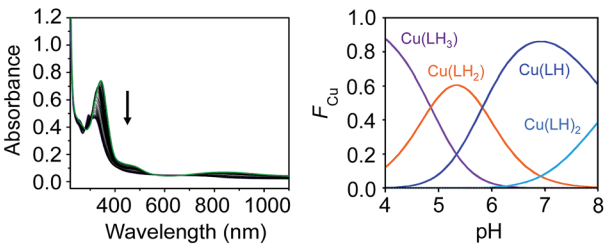

			logβ^a
Cu + L	⟷	Cu(L)	7.1(3)[b]
Cu + 2L	⟷	$Cu(L)_2$	17.1(9)[b]
Cu + LH	⟷	Cu(LH)	30.8(5)
Cu + 2LH	⟷	$Cu(LH)_2$	48.8(7)
Cu + LH_2	⟷	$Cu(LH_2)$	36.6(8)
Cu + $2LH_2$	⟷	$Cu(LH_2)_2$	57.7(5)[b]
Cu + LH_3	⟷	$Cu(LH_3)$	41.5(4)
Cu + $2LH_3$	⟷	$Cu(LH_3)_2$	63.5(5)[b]

Fig. 4 Solution speciation studies of Cu(II)–**4** complexes. Top: variable-pH UV-Vis titration spectra (left) and solution speciation diagram (right) for Cu(II)–**4** (F_{Cu} = fraction of species in solution relative to Cu(II)). Bottom: summary of solution equilibria and stability constants (log β). Experimental conditions: [$CuCl_2$] = 15 μM, [**4**] = 30 μM; pH 8; I = 0.1 M NaCl; room temperature. Charges are omitted for clarity. [a] The error in the last digit is shown in parentheses. [b] Cu(L), $Cu(L)_2$, $Cu(LH_2)_2$, and $Cu(LH_3)_2$ were introduced in the calculation to provide the best fit to the data, but contributed a negligible amount to the overall solution speciation.

Interaction of aminoisoflavones with Aβ species

The interaction between aminoisoflavones and Aβ species in solution was investigated by isothermal titration calorimetry (ITC), NMR, and docking studies. ITC was first used to measure thermodynamic parameters for the interaction of Aβ with **1**, **2**, and **4** (Table S1†). Using a sequential binding model with one identical site to fit the data, these ligands were found to bind to $A\beta_{40}$ with *ca.* low mM affinity ($K_A = 6.8\ (\pm 3.0) \times 10^4$, 7.9 ($\pm$2.9) $\times 10^3$, and $3.2 \pm (0.7) \times 10^3\ M^{-1}$ for **1**, **2**, and **4**, respectively) and with favorable values of Gibbs free energy ($\Delta G = -27.3\ (\pm 1.1)$, $-22.2\ (\pm 0.9)$, and $-19.9\ (\pm 0.6)$ kJ mol^{-1} for **1**, **2**, and **4**, respectively) (Table S1†). Different peptide–ligand interactions, however, likely accounted for favorable binding. For **1**, which lacks the catechol moiety, entropic contributions ($-T\Delta S = -38.7\ (\pm 1.6)$ kJ mol^{-1}) were greater than enthalpic contributions ($\Delta H = 11.3\ (\pm 1.2)$ kJ mol^{-1}). Conversely, the enthalpic term for **4** is large and negative in magnitude ($\Delta H = -116.3\ (\pm 19.6)$ kJ mol^{-1}), while the contribution from entropy is unfavorable ($-T\Delta S = 96.4\ (\pm 19.6)$ kJ mol^{-1}). Similar to **4**, compound **2** showed favorable enthalpic ($\Delta H = -59.1\ (\pm 22.6)$ kJ mol^{-1}) and unfavorable entropic ($-T\Delta S = 36.9\ (\pm 22.6)$ kJ mol^{-1}) contributions (Table S1†).

The thermodynamic parameters governing these peptide–small molecule interactions can be related to the variations in their chemical structures. Since **1** is distinguished from **2** or **4** by the absence of a catechol moiety for metal binding, it is reasonable to expect that these molecules may favor dissimilar interactions with the peptide. Compound **1** contains an unsubstituted phenyl ring, which might suggest that the interactions are mainly driven by hydrophobic interaction with the peptide; these types of interactions usually translate to an increase in the entropy as measured by ITC.[37] On the other hand, **4** would potentially facilitate the formation of hydrogen bonding contacts between the molecule and the peptide in solution due to the *o*-dihydroxy groups from the catechol moiety, resulting in favorable interaction indicated by the large, negative ΔH value.[37] Compound **2**, which has a catechol group in the B ring but has no functionality on the A ring, presented a similar result to **4**, indicating that these molecules interact with Aβ similarly due to the presence of the catechol group which facilitates mainly hydrophilic contacts. Despite distinctive, direct contacts predicted with the peptide for **1** compared to **2** and **4**, each of these molecules have favorable Gibbs free energy values that could be used to rationalize their ability to interact with metal-free Aβ species (*vide infra*). The ITC results suggest that **1**, **2**, and **4** bind $A\beta_{40}$. The mechanism of peptide binding with each compound, however, appears to differ with the relative balance of enthalpic and entropic contributions.

Accordingly, the binding of compounds **1** and **4** to $A\beta_{40}$ was subjected to further analysis by NMR. Previously, we have shown that monomeric $A\beta_{40}$ can adopt a 3_{10} helical structure in the central hydrophobic region at moderate ionic strength and low temperature (PDB ID 2LFM).[38] Using similar conditions, the regions of $A\beta_{40}$ potentially capable of interacting with the aminoisoflavones were mapped. Changes in the SOFAST-HMQC spectra (SOFAST = 2D band-selective optimized flip-angle short transient; HMQC = heteronuclear multiple quantum correlation) of freshly dissolved $A\beta_{40}$ upon titration with **1** and **4** suggested potential interaction of the compounds with three peptide sites (Fig. 5 and 6). The chemical shift perturbations were slightly larger for **1** (Fig. 5a and 6b) than **4** (Fig. 5b and 6c), in agreement with the larger free energy change upon binding to $A\beta_{40}$ for compound **1**, as measured by ITC. Moderate (0.02–0.15 ppm on the scaled chemical shift scale) chemical shift perturbations were detected for both compounds in two specific regions of the peptide near the N-terminus (R5-S8) and the N-terminal part of the 3_{10} helix (H13-L17) (Fig. 6a). These two regions are close together in the $A\beta_{40}$ structure (Fig. 6d) and appear to form a potential binding site for the compounds and/or be rearranged upon interaction with the compounds. A third area of chemical shift perturbation is closer to the C-terminus (M35-V40). The chemical shifts near the C-terminus may reflect either the rearrangement of the disordered C-terminus to pack against the aminoisoflavone or may be an indication of a second lower affinity binding site. The perturbation of the chemical shifts on specific residues of $A\beta_{40}$ by aminoisoflavones was notably different than that observed with the related catechol EGCG with $A\beta_{40}$ and α-synuclein, where large nearly

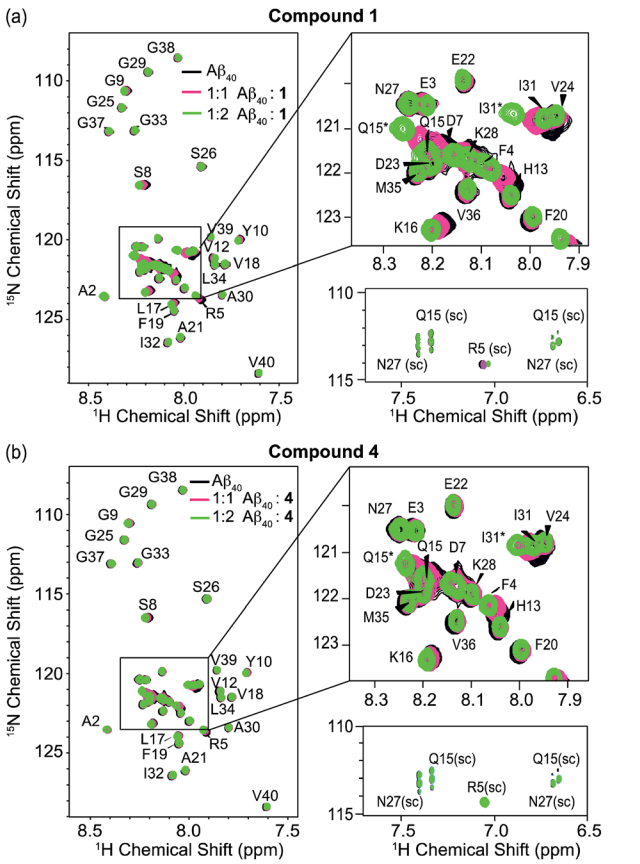

Fig. 5 Interaction of **1** and **4** with freshly dissolved $A\beta_{40}$ at near stoichiometric ratios. SOFAST-HMQC spectra of 80 μM freshly dissolved $A\beta_{40}$ in 20 mM deuterated Tris (pH 7.4) with 50 mM NaCl and 10% D_2O, then titrated with (a) **1** and (b) **4** to the indicated molar ratios at 4 °C. Chemical shift perturbations were detected primarily for the amide resonances R5-S8 and H13-L17 (see Fig. 6).

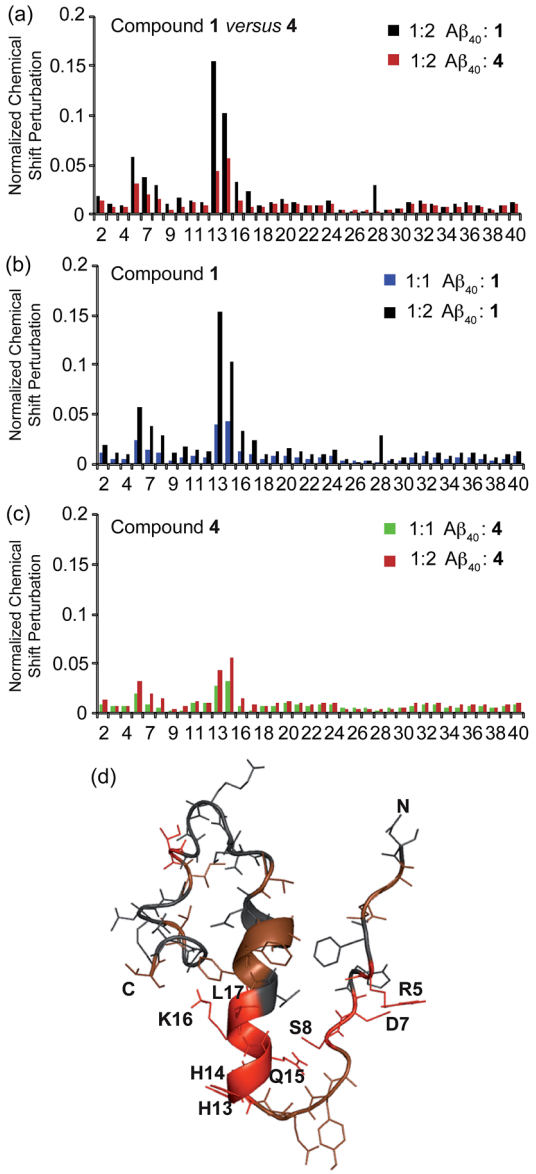

Fig. 6 Chemical shift changes in $A\beta_{40}$ induced by **1** and **4**. (a) Chemical shift perturbations for $A\beta_{40}$ in the presence of **1** or **4** (1 : 2 molar ratio). The normalized chemical shift perturbation is equivalent to $\sqrt{(\Delta^1H)^2 + \frac{(\Delta^{15}N)^2}{\sqrt{5}}}$. Normalized chemical shift perturbations for (b) **1** and (c) **4**. (d) Residues with the largest chemical shift perturbations mapped onto the NMR structure of $A\beta_{40}$ (PDB 2LFM). The residues with the largest chemical shift perturbations (>0.02 ppm) are indicated in red; residues with smaller chemical shift perturbations (0.01–0.02 ppm) are presented in brown.

uniform decreases in intensity had been observed, suggesting non-specific binding,[12b,14,39] and indicates that polyphenols do not have a single uniform mechanism of binding.[23]

To visualize the potential contacts of **1**, **2**, and **4** with $A\beta_{40}$, flexible ligand docking studies were employed using the solution NMR structure of metal-free $A\beta_{40}$ (PDB 2LFM) (Fig. S7†).[38] The docked conformations of these ligands with the peptide were generally found in similar positions around the peptide, situated nearer to the N-terminus or 3_{10}-helix, consistent with the chemical shift perturbations observed by NMR and the previous results obtained with the structurally related catechin, EGCG.[12b] Interaction near the N-terminus of $A\beta_{40}$ is desirable because the residues that bind Cu(II) and Zn(II) exist in this portion of the sequence, while interaction with the helical portion of the peptide could be beneficial in order to hinder the initial stages of self-association in this region (L17-A21).[1b–e]

The similarity in the pattern of the chemical shift perturbations suggests that **1** and **4** bind to the same site in $A\beta_{40}$ (Fig. 6). Although the compounds also often preferred similar binding modes in the docking studies, there were some slight deviations among the results that could support the findings from ITC. For example, there were a few instances where **4** was oriented in a more favourable position to facilitate hydrogen bonding contacts, while in some conformations **1** was more aligned with the helical portion of the peptide. Compound **2** could dock in similar positions to both ligands, as expected based on its structure, with most expected conformations being situated near the N-terminus in the area preceding the helical portion of the peptide, similar to the NMR results obtained for **1**. Although the overall view of the ligand interactions with $A\beta_{40}$ from NMR and docking is relatively consistent with the ITC results, the magnitude of the interactions cannot be completely determined from either technique. As noted above, only moderate chemical shift perturbations were detected for specific regions of $A\beta_{40}$ at 1 : 1 and 1 : 2 protein-to-ligand molar ratios. At higher concentrations of compound **1** ($A\beta_{40}$: **1** = 1 : 5), much larger changes in chemical shift were observed, along with a strong reduction in intensity (Fig. 7). The changes in chemical shift did not appear to match the pattern obtained at lower concentrations of **1**, although for many residues a definite assignment could not be made. Two new negative (folded) broad peaks were also apparent in the SOFAST-HMQC spectra, within the side-chain region of the spectra below 7.5 ppm. The appearance of a new species at higher ligand concentrations was also supported

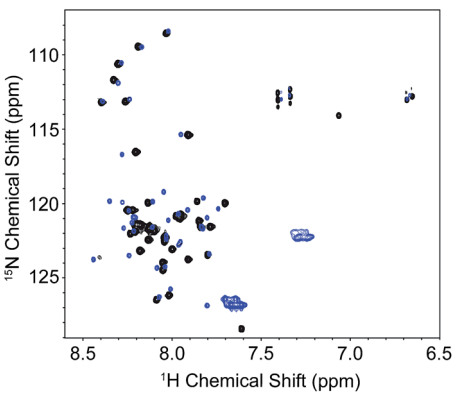

Fig. 7 Interaction of $A\beta_{40}$ with 5 equiv. of **1**. SOFAST-HMQC spectra of 80 μM freshly dissolved $A\beta_{40}$ (black) in 20 mM deuterated Tris (pH 7.4) with 50 mM NaCl and 10% D_2O, and with 5 equiv. of **1** (blue) at 4 °C. Large chemical shift changes indicate that a global change in conformation has taken place, possibly due to the formation of covalent adducts.

by a strong new peak at 7.64 ppm and three weaker doublets at 6.77, 6.83, and 6.89 ppm in the ^{1}H spectrum of the ligand (Fig. S8†). The intensity changes were not accompanied by the increase in linewidth that would be expected for exchange broadening, suggesting that some of the peptide was lost instead to aggregation. The dramatic changes in the SOFAST-HMQC spectra suggest that either a global conformational change favoring aggregation may have taken place, or compound **1** may have covalently attached to the peptide through Schiff base formation as has been observed previously with other flavonoids.[40]

In addition to binding to freshly dissolved $A\beta_{40}$, compounds **1** and **4** may have the capability to bind to other forms of $A\beta_{40}$, such as fibrils. To probe these possible interactions, we employed saturation transfer difference (STD) NMR experiments to map the regions of the ligand which bind preformed fibrils of $A\beta_{40}$ (Fig. 8).[10p,41] To visualize the potential contacts of **4** with Aβ fibrils, flexible ligand docking studies were employed with the solid state NMR structure of metal-free $A\beta_{40}$ (PDB 2LMN and 2LMO) (Fig. 8c, S9, and S10†).[42] The normalized signal strengths (STD/STD reference) corresponding to each ligand atom are proportional to its proximity to the amyloid fibril, allowing an atomic-level map of the binding interactions from the ligand to the Aβ fibril to be made.[10p,41] The results from the STD NMR experiments indicate that both **1** and **4** interact fairly strongly (mM to μM dissociation constant) with the fibril and elicit a relatively strong STD signal (approximately 4.5% (for **1**) and 5.9% (for **4**) of the reference signal at a 3 s saturation power of 50 dB, similar in magnitude to previous results with other catechols[41]). The STD results also suggest that **1** and **4** bind similarly to the Aβ fibril (Fig. 8b).

The STD effect was distributed relatively evenly throughout both compounds, implying that the entire molecule could be packed to some degree against the fibril. In both compounds the strongest interaction is at carbon 8 on the A ring, suggesting the ketone is pointing away from the fibril in both compounds. While the STD patterns were overall similar, carbon 2′ in the B ring in **4** was shown to have a significantly higher STD effect than the corresponding carbon in **1**. The increased effect in this region is an indication that the presence of the catechol group causes a reorientation of **4** to put the B ring in closer contact with the fibril, which may explain the somewhat higher affinity of **4** over **1** for the Aβ fibril. This binding mode is supported by and visualized by simulated docking of **4** with Aβ fibers (PDB 2LMO and 2LMN).[42] Consistent with the result from STD NMR, the calculated lowest energy conformation (Fig. 8c) predicted that ring A and B are close to two residues of D23 from adjacent single β strands. These residues were positioned within effective hydrogen bonding distance of the hydroxyl moieties of **4**, and their potential hydrogen bonding may stabilize this conformation. In addition, the aromatic rings A and B were docked to face two hydrophobic I32 residues. Furthermore, the amino group was toward the loop motif which is a solvent accessible region. The best fit conformation of **4**, intervening between β sheets around the loop region, will allow effective hydrogen bonding and hydrophobic interaction with some residues of the peptides.

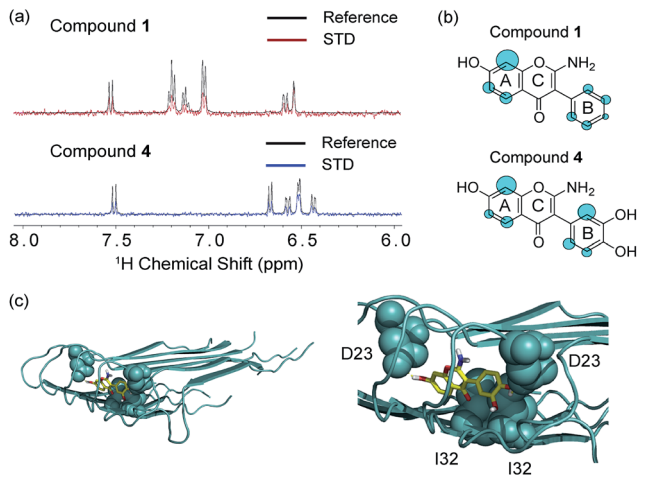

Fig. 8 Interaction of **1** and **4** with $A\beta_{40}$ fibrils by STD NMR. (a) STD NMR spectra of **1** and **4** at 10 : 1 ligand to peptide ratio using pre-assembled $A\beta_{40}$ fibrils. A comparison of STD signal intensity to the STD reference reflects the relative proximity of the corresponding proton to the $A\beta_{40}$ fibril. (b) Normalized STD intensities mapped onto each compound structure. Larger blue circles indicate a more intense STD effect. Note that the hydroxyl and amine protons were not detected by this experiment. (c) Lowest energy docked conformation of **4** to the $A\beta_{40}$ fiber (PDB 2LMO)[42] (right: an expanded view of **4**'s binding site). Residues within effective hydrogen boding distance from **4** were indicated as spheres. Other docked conformations and corresponding energies are summarized in Fig. S9 and S10.†

Antioxidant properties

The Trolox antioxidant equivalence capacity (TEAC) assay[43] was conducted to investigate the radical scavenging capability of our aminoisoflavones (Fig. S11†).[44] Compared to the vitamin E analogue Trolox, **3** was approximately three times more effective at quenching the radical ($ABTS^{+}$). Compounds **2** and **4** could also reduce the amount of the radical in solution to a similar extent as Trolox. Among the aminoisoflavones, **1** showed the lowest TEAC value, suggesting its limited utility as a radical scavenger. Structurally, the most likely radical scavengers among these molecules contain the catechol moiety and may be able to support the resulting ligand intermediate (*e.g.*, semiquinone) upon donation of a hydrogen atom to the organic radical; the absence of the catechol moiety in **1** may preclude its formation of a stable intermediate upon interacting with $ABTS^{+}$.[44a] To account for their lower TEAC values compared to that of **3**, the possibility for resonance stabilization of **2** and **4** might make them less capable of hydrogen atom donation; the Cl atom in **3** may be capable of producing a radical that could also quench the $ABTS^{+}$.[44a]

Conclusions

Advancement in the AD research field has been challenged by the lack of cohesive evidence to explain the origins of the disease. It has been suggested that the formerly competing hypotheses (*i.e.*, metal ion and amyloid cascade) are

intertwined. In order to target these two potential pathological factors, efforts have been made to investigate molecules with multiple functions, including metal chelation and Aβ interaction, in hopes of devising a comprehensive structure–interaction–reactivity relationship to govern designs of new chemical tools and/or therapeutics. For this purpose, the flavonoid framework has been identified as a potential avenue, as multiple flavonoids inherently have structural components for interacting with metal ions and Aβ.[12a,b] In the present study, the flavonoid framework was successfully applied to a synthetic design strategy to generate the aminoisoflavones **1–4**. Previous work has shown that using flavonoid derivatives, designed with slight modification of the parent natural product framework, led to significant impact upon reactivity (*i.e.*, no reactivity observed).[10f] The aminoisoflavones reported herein demonstrated reactivity, even with alterations upon the flavonoid base scaffold. The inclusion of the catechol group with the unnatural primary amine was shown to impart noticeable properties for interaction and reactivity with metals, Aβ, and/or metal–Aβ (*i.e.*, metal chelation, hydrophilic and hydrophobic contacts with Aβ peptides) while additional functional groups (*i.e.*, OH, Cl) did not significantly perturb these properties. This suggests that the catechol moiety may be required to achieve a balance in interaction with metal ions and/or Aβ, as well as influence Aβ aggregation in the absence and presence of metal ions. Furthermore, the catechol moiety was shown to be potentially important for the interaction between ligands and metal–Aβ species. In addition, the catechol group seems to offer other potentially useful properties, such as radical scavenging activity. Thus, this work demonstrates that the flavonoids can be manipulated into simple structures to tune chemical properties (*i.e.*, metal binding, Aβ interaction) and, subsequently, *in vitro* reactivity toward metal-free Aβ and metal–Aβ aggregation, which offers preliminary insights into the structure–interaction–reactivity relationship of flavonoid structures with Aβ and metal–Aβ species.

Acknowledgements

This work was supported by the Ministero dell'Università e della Ricerca PRIN2010-2011, Prot. no. 20105YY2HL_006 (to S.M.) and PRIN2010-2011, Prot. no. 20105YY2HL_002 (to G.B.), the National Institutes of Health (GM-084018) (to A.R.), the Ruth K. Broad Biomedical Foundation, the National Science Foundation (CHE-1253155), the DGIST R&D Program of the Ministry of Science, ICT and Future Planning of Korea (14-BD-0403), and the 2013 Research Fund (Project number 1.130068.01) of UNIST (Ulsan National Institute of Science and Technology) (to M.H.L.). D.L. acknowledges support from the Basic Science program through the National Research Foundation of Korea funded by the Ministry of Education, Science, and Technology (2009-0087836). A.S.D. is grateful to the National Science Foundation for a Graduate Research Fellowship. A.K. thanks the Department of Chemistry at the University of Michigan for a Research Excellence Fellowship. We acknowledge Michael Beck for assistance with docking studies.

Notes and references

1 (*a*) Alzheimer's Association, *Alzheimer's Dementia*, 2012, **8**, 131–168; (*b*) A. S. DeToma, S. Salamekh, A. Ramamoorthy and M. H. Lim, *Chem. Soc. Rev.*, 2012, **41**, 608–621; (*c*) A. S. Pithadia and M. H. Lim, *Curr. Opin. Chem. Biol.*, 2012, **16**, 67–73; (*d*) M. G. Savelieff, S. Lee, Y. Liu and M. H. Lim, *ACS Chem. Biol.*, 2013, **8**, 856–865; (*e*) K. P. Kepp, *Chem. Rev.*, 2012, **112**, 5193–5239.

2 (*a*) C. Soto, *Nat. Rev. Neurosci.*, 2003, **4**, 49–60; (*b*) D. B. Teplow, N. D. Lazo, G. Bitan, S. Bernstein, T. Wyttenbach, M. T. Bowers, A. Baumketner, J.-E. Shea, B. Urbanc, L. Cruz, J. Borreguero and H. E. Stanley, *Acc. Chem. Res.*, 2006, **39**, 635–645; (*c*) A. Rauk, *Chem. Soc. Rev.*, 2009, **38**, 2698–2715.

3 (*a*) J. Hardy and D. J. Selkoe, *Science*, 2002, **297**, 353–356; (*b*) R. Jakob-Roetne and H. Jacobsen, *Angew. Chem., Int. Ed.*, 2009, **48**, 3030–3059; (*c*) S. Ayton, P. Lei and A. I. Bush, *Free Radical Biol. Med.*, 2013, **62**, 76–89.

4 (*a*) C. A. Ross and M. A. Poirier, *Nat. Med.*, 2004, (suppl. 10), S10–S17; (*b*) M. Fändrich, *Cell. Mol. Life Sci.*, 2007, **64**, 2066–2078.

5 (*a*) X. Zhu, B. Su, X. Wang, M. A. Smith and G. Perry, *Cell. Mol. Life Sci.*, 2007, **64**, 2202–2210; (*b*) P. Faller and C. Hureau, *Chem.–Eur. J.*, 2012, **18**, 15910–15920; (*c*) M. A. Greenough, J. Camakaris and A. I. Bush, *Neurochem. Int.*, 2013, **62**, 540–555; (*d*) G. Eskici and P. H. Axelsen, *Biochemistry*, 2012, **51**, 6289–6311; (*e*) P. Faller and C. Hureau, *Dalton Trans.*, 2009, 1080–1094; (*f*) P. Faller, *ChemBioChem*, 2009, **10**, 2837–2845.

6 A. I. Bush, *J. Alzheimer's Dis.*, 2013, **33**(suppl. 1), S277–S281.

7 (*a*) J. Shearer and V. A. Szalai, *J. Am. Chem. Soc.*, 2008, **130**, 17826–17835; (*b*) J. Shearer, P. E. Callan, T. Tran and V. A. Szalai, *Chem. Commun.*, 2010, **46**, 9137–9139; (*c*) C. Ghosh and S. G. Dey, *Inorg. Chem.*, 2013, **52**, 1318–1327; (*d*) F. Bousejra-ElGarah, C. Bijani, Y. Coppel, P. Faller and C. Hureau, *Inorg. Chem.*, 2011, **50**, 9024–9030.

8 (*a*) C. J. Sarell, S. R. Wilkinson and J. H. Viles, *J. Biol. Chem.*, 2010, **285**, 41533–41540; (*b*) D. Noy, I. Solomonov, O. Sinkevich, T. Arad, K. Kjaer and I. Sagi, *J. Am. Chem. Soc.*, 2008, **130**, 1376–1383.

9 P. Faller, *Free Radical Biol. Med.*, 2012, **52**, 747–748.

10 (*a*) C. Rodríguez-Rodríguez, M. Telpoukhovskaia and C. Orvig, *Coord. Chem. Rev.*, 2012, **256**, 2308–2332; (*b*) M. G. Savelieff, A. S. DeToma, J. S. Derrick and M. H. Lim, *Acc. Chem. Res.*, 2014, **47**, 2475–2482; (*c*) C. Hureau, I. Sasaki, E. Gras and P. Faller, *ChemBioChem*, 2010, **11**, 950–953; (*d*) A. Dedeoglu, K. Cormier, S. Payton, K. A. Tseitlin, J. N. Kremsky, L. Lai, X. Li, R. D. Moir, R. E. Tanzi, A. I. Bush, N. W. Kowall, J. T. Rogers and X. Huang, *Exp. Gerontol.*, 2004, **39**, 1641–1649; (*e*) W.-h. Wu, P. Lei, Q. Liu, J. Hu, A. P. Gunn, M.-s. Chen, W.-f. Rui, X.-y. Su, Z.-p. Xie, Y.-F. Zhao, A. I. Bush and Y.-m. Li, *J. Biol. Chem.*, 2008, **283**, 31657–31664; (*f*) C. Rodríguez-Rodríguez, N. Sánchez de Groot, A. Rimola, Á. Álvarez-Larena, V. Lloveras, J. Vidal-Gancedo, S. Ventura,

J. Vendrell, M. Sodupe and P. González-Duarte, *J. Am. Chem. Soc.*, 2009, **131**, 1436–1451; (*g*) S. S. Hindo, A. M. Mancino, J. J. Braymer, Y. Liu, S. Vivekanandan, A. Ramamoorthy and M. H. Lim, *J. Am. Chem. Soc.*, 2009, **131**, 16663–16665; (*h*) J.-S. Choi, J. J. Braymer, R. P. R. Nanga, A. Ramamoorthy and M. H. Lim, *Proc. Natl. Acad. Sci. U. S. A.*, 2010, **107**, 21990–21995; (*i*) J.-S. Choi, J. J. Braymer, S. K. Park, S. Mustafa, J. Chae and M. H. Lim, *Metallomics*, 2011, **3**, 284–291; (*j*) J. J. Braymer, J.-S. Choi, A. S. DeToma, C. Wang, K. Nam, J. W. Kampf, A. Ramamoorthy and M. H. Lim, *Inorg. Chem.*, 2011, **50**, 10724–10734; (*k*) A. S. Pithadia, A. Kochi, M. T. Soper, M. W. Beck, Y. Liu, S. Lee, A. S. DeToma, B. T. Ruotolo and M. H. Lim, *Inorg. Chem.*, 2012, **51**, 12959–12967; (*l*) X. He, H. M. Park, S. J. Hyung, A. S. DeToma, C. Kim, B. T. Ruotolo and M. H. Lim, *Dalton Trans.*, 2012, **41**, 6558–6566; (*m*) A. K. Sharma, S. T. Pavlova, J. Kim, D. Finkelstein, N. J. Hawco, N. P. Rath, J. Kim and L. M. Mirica, *J. Am. Chem. Soc.*, 2012, **134**, 6625–6636; (*n*) M. R. Jones, E. L. Service, J. R. Thompson, M. C. P. Wang, I. J. Kimsey, A. S. DeToma, A. Ramamoorthy, M. H. Lim and T. Storr, *Metallomics*, 2012, **4**, 910–920; (*o*) Y. Liu, A. Kochi, A. S. Pithadia, S. Lee, Y. Nam, M. W. Beck, X. He, D. Lee and M. H. Lim, *Inorg. Chem.*, 2013, **52**, 8121–8130; (*p*) S. Lee, X. Zheng, J. Krishnamoorthy, M. G. Savelieff, H. M. Park, J. R. Brender, J. H. Kim, J. S. Derrick, A. Kochi, H. J. Lee, C. Kim, A. Ramamoorthy, M. T. Bowers and M. H. Lim, *J. Am. Chem. Soc.*, 2014, **136**, 299–310.

11 (*a*) M. Ono, M. Haratake, H. Saji and M. Nakayama, *Bioorg. Med. Chem.*, 2008, **16**, 6867–6872; (*b*) M. Ono, Y. Maya, M. Haratake and M. Nakayama, *Bioorg. Med. Chem.*, 2007, **15**, 444–450; (*c*) M. Ono, M. Hori, M. Haratake, T. Tomiyama, H. Mori and M. Nakayama, *Bioorg. Med. Chem.*, 2007, **15**, 6388–6396; (*d*) M. Ono, R. Watanabe, H. Kawashima, T. Kawai, H. Watanabe, M. Haratake, H. Saji and M. Nakayama, *Bioorg. Med. Chem.*, 2009, **17**, 2069–2076; (*e*) H. F. Kung, C. W. Lee, Z. P. Zhuang, M. P. Kung, C. Hou and K. Plossl, *J. Am. Chem. Soc.*, 2001, **123**, 12740–12741; (*f*) W. Zhang, S. Oya, M. P. Kung, C. Hou, D. L. Maier and H. F. Kung, *J. Med. Chem.*, 2005, **48**, 5980–5988; (*g*) M.-P. Kung, C. Hou, Z.-P. Zhuang, B. Zhang, D. Skovronsky, J. Q. Trojanowski, V. M.-Y. Lee and H. F. Kung, *Brain Res.*, 2002, **956**, 202–210; (*h*) W. E. Klunk, Y. Wang, G. F. Huang, M. L. Debnath, D. P. Holt and C. A. Mathis, *Life Sci.*, 2001, **69**, 1471–1484; (*i*) M. Ono, H. Watanabe, R. Watanabe, M. Haratake, M. Nakayama and H. Saji, *Bioorg. Med. Chem. Lett.*, 2011, **21**, 117–120.

12 (*a*) A. S. DeToma, J.-S. Choi, J. J. Braymer and M. H. Lim, *ChemBioChem*, 2011, **12**, 1198–1201; (*b*) S.-J. Hyung, A. S. DeToma, J. R. Brender, S. Lee, S. Vivekanandan, A. Kochi, J.-S. Choi, A. Ramamoorthy, B. T. Ruotolo and M. H. Lim, *Proc. Natl. Acad. Sci. U. S. A.*, 2013, **110**, 3743–3748; (*c*) W. M. Tay, G. F. da Silva and L. J. Ming, *Inorg. Chem.*, 2013, **52**, 679–690.

13 (*a*) B. H. Havsteen, *Pharmacol. Ther.*, 2002, **96**, 67–202; (*b*) L. H. Yao, Y. M. Jiang, J. Shi, F. A. Tomas-Barberan, N. Datta, R. Singanusong and S. S. Chen, *Plant Foods Hum. Nutr.*, 2004, **59**, 113–122; (*c*) J. Kim, H. J. Lee and K. W. Lee, *J. Neurochem.*, 2010, **112**, 1415–1430.

14 D. E. Ehrnhoefer, J. Bieschke, A. Boeddrich, M. Herbst, L. Masino, R. Lurz, S. Engemann, A. Pastore and E. E. Wanker, *Nat. Struct. Mol. Biol.*, 2008, **15**, 558–566.

15 M. Hirohata, K. Ono, J. Takasaki, R. Takahashi, T. Ikeda, A. Morinaga and M. Yamada, *Biochim. Biophys. Acta*, 2012, **1822**, 1316–1324.

16 (*a*) E. Middleton Jr, C. Kandaswami and T. C. Theoharides, *Pharmacol. Rev.*, 2000, **52**, 673–751; (*b*) R. J. Nijveldt, E. van Nood, D. E. C. van Hoorn, P. G. Boelens, K. van Norren and P. A. M. van Leeuwen, *Am. J. Clin. Nutr.*, 2001, **74**, 418–425.

17 (*a*) A. E. Martell and R. M. Smith, *Critical Stability Constants*, Plenum, New York, 1974–1989; (*b*) N. Schweigert, A. J. Zehnder and R. I. Eggen, *Environ. Microbiol.*, 2001, **3**, 81–91; (*c*) A. Avdeef, S. R. Sofen, T. L. Bregante and K. N. Raymond, *J. Am. Chem. Soc.*, 1978, **100**, 5362–5370; (*d*) J. F. Severino, B. A. Goodman, T. G. Reichenauer and K. F. Pirker, *Free Radical Res.*, 2011, **45**, 115–124; (*e*) D. R. Eaton, *Inorg. Chem.*, 1964, **3**, 1268–1271; (*f*) W. Kaim, *Dalton Trans.*, 2003, 761–768.

18 J. McMurry, *Organic Chemistry*, Brooks/Cole–Thomson Learning, Belmont, CA, 6th edn, 2004.

19 (*a*) R. J. Wall, G. He, M. S. Denison, C. Congiu, V. Onnis, A. Fernandes, D. R. Bell, M. Rose, J. C. Rowlands, G. Balboni and I. R. Mellor, *Toxicology*, 2012, **297**, 26–33; (*b*) G. Balboni, C. Congiu, V. Onnis, A. Maresca, A. Scozzafava, J. Y. Winum, A. Maietti and C. T. Supuran, *Bioorg. Med. Chem. Lett.*, 2012, **22**, 3063–3066.

20 B. G. Jang, S. M. Yun, K. Ahn, J. H. Song, S. A. Jo, Y. Y. Kim, D. K. Kim, M. H. Park, C. Han and Y. H. Koh, *J. Alzheimer's Dis.*, 2010, **21**, 939–945.

21 R. Leuma Yona, S. Mazeres, P. Faller and E. Gras, *ChemMedChem*, 2008, **3**, 63–66.

22 (*a*) A. M. Mancino, S. S. Hindo, A. Kochi and M. H. Lim, *Inorg. Chem.*, 2009, **48**, 9596–9598; (*b*) M. T. Soper, A. S. DeToma, S.-J. Hyung, M. H. Lim and B. T. Ruotolo, *Phys. Chem. Chem. Phys.*, 2013, **15**, 8952–8961.

23 A. R. Ladiwala, J. S. Dordick and P. M. Tessier, *J. Biol. Chem.*, 2011, **286**, 3209–3218.

24 (*a*) J. Bieschke, J. Russ, R. P. Friedrich, D. E. Ehrnhoefer, H. Wobst, K. Neugebauer and E. E. Wanker, *Proc. Natl. Acad. Sci. U. S. A.*, 2010, **107**, 7710–7715; (*b*) J. A. Lemkul and D. R. Bevan, *Biochemistry*, 2012, **51**, 5990–6009.

25 S. Yun, B. Urbanc, L. Cruz, G. Bitan, D. B. Teplow and H. E. Stanley, *Biophys. J.*, 2007, **92**, 4064–4077.

26 (*a*) J. J. Braymer, N. M. Merrill and M. H. Lim, *Inorg. Chim. Acta*, 2012, **380**, 261–268; (*b*) T. Storr, M. Merkel, G. X. Song-Zhao, L. E. Scott, D. E. Green, M. L. Bowen, K. H. Thompson, B. O. Patrick, H. J. Schugar and C. Orvig, *J. Am. Chem. Soc.*, 2007, **129**, 7453–7463.

27 http://www.acdlabs.com.

28 H. Pajouhesh and G. R. Lenz, *NeuroRx*, 2005, **2**, 541–553.

29 (*a*) R. C. Hider, Z. D. Liu and H. H. Khodr, *Methods Enzymol.*, 2001, **335**, 190–203; (*b*) M. Satterfield and J. S. Brodbelt, *Anal. Chem.*, 2000, **72**, 5898–5906.

30 M. J. Sever and J. J. Wilker, *Dalton Trans.*, 2004, 1061–1072.
31 C. A. Tyson and A. E. Martell, *J. Am. Chem. Soc.*, 1968, **90**, 3379–3386.
32 P. Verma, J. Weir, L. Mirica and T. D. Stack, *Inorg. Chem.*, 2011, **50**, 9816–9825.
33 D. Maity, A. K. Manna, D. Karthigeyan, T. K. Kundu, S. K. Pati and T. Govindaraju, *Chemistry*, 2011, **17**, 11152–11161.
34 T. Kundu, B. Sarkar, T. K. Mondal, S. M. Mobin, F. A. Urbanos, J. Fiedler, R. Jiménez-Aparicio, W. Kaim and G. K. Lahiri, *Inorg. Chem.*, 2011, **50**, 4753–4763.
35 J. Balla, T. Kiss and R. F. Jameson, *Inorg. Chem.*, 1992, **31**, 58–62.
36 J. S. Thompson and J. C. Calabrese, *J. Am. Chem. Soc.*, 1986, **108**, 1903–1907.
37 S. H. Wang, F. F. Liu, X. Y. Dong and Y. Sun, *J. Phys. Chem. B*, 2010, **114**, 11576–11583.
38 S. Vivekanandan, J. R. Brender, S. Y. Lee and A. Ramamoorthy, *Biochem. Biophys. Res. Commun.*, 2011, **411**, 312–316.
39 S. Sinha, Z. Du, P. Maiti, F. G. Klarner, T. Schrader, C. Wang and G. Bitan, *ACS Chem. Neurosci.*, 2012, **3**, 451–458.
40 (*a*) N. Popovych, J. R. Brender, R. Soong, S. Vivekanandan, K. Hartman, V. Basrur, P. M. Macdonald and A. Ramamoorthy, *J. Phys. Chem. B*, 2012, **116**, 3650–3658; (*b*) M. Zhu, S. Rajamani, J. Kaylor, S. Han, F. Zhou and A. L. Fink, *J. Biol. Chem.*, 2004, **279**, 26846–26857; (*c*) F. L. Palhano, J. Lee, N. P. Grimster and J. W. Kelly, *J. Am. Chem. Soc.*, 2013, **135**, 7503–7510.
41 C. Airoldi, E. Sironi, C. Dias, F. Marcelo, A. Martins, A. P. Rauter, F. Nicotra and J. Jimenez-Barbero, *Chem.–Asian J.*, 2013, **8**, 596–602.
42 A. T. Petkova, W.-M. Yau and R. Tycko, *Biochemistry*, 2006, **45**, 498–512.
43 The $ABTS^{+}$ radicals employed in the TEAC assay do not represent ROS, such as hydroxyl radicals.
44 (*a*) C. A. Rice-Evans, N. J. Miller and G. Paganga, *Free Radical Biol. Med.*, 1996, **20**, 933–956; (*b*) R. Re, N. Pellegrini, A. Proteggente, A. Pannala, M. Yang and C. Rice-Evans, *Free Radical Biol. Med.*, 1999, **26**, 1231–1237.